

Article

Model-Based Design of LFP Battery Thermal Management System for EV Application

Nadjiba Sophy-Mahfoudi ^{1,*}, Sai-Vandhan Sekharam ¹, M'hamed Boutaous ²  and Shihe Xin ²

¹ Université de Bourgogne, DRIVE, 49 rue Mademoiselle Bourgeois, 58000 Nevers, France; sekham.vandhan@gmail.com

² Université de Lyon, CNRS, INSA-Lyon, CETHIL, 9 rue de la physique, Campus LyonTech la Doua, 96621 Villeurbanne, France; mhamed.boutaous@insa-lyon.fr (M.B.); shihe.xin@insa-lyon.fr (S.X.)

* Correspondence: nadjiba.sophy@u-bourgogne.fr

Abstract: This study uses an equivalent circuit model (ECM) and real-time data to model lithium iron phosphate (LFP) batteries to accurately represent their thermo-electrical behavior. In particular, the focus is on a thermal management perspective in high-performance electric vehicles (EVs). The ECM-based battery management system, which effectively captures the non-linear behavior of Li-ion batteries, is developed to optimize the safety, lifespan and overall performance of the EV battery management system. The ECM-based battery model is validated using real-time drive cycle data to enhance the understanding of battery management systems, contributing to improved overall performance and reliability. In addition, advanced estimation algorithms, such as the extended Kalman filter, are integrated to further improve the predictive capabilities of battery parameters. Battery terminal voltage prediction with an average RMSE error of 0.015% is achieved, highlighting the critical role of ECMs and advanced numerical simulation methods in optimizing the performance of automotive battery management systems. The achieved results provide important guidance for model-based design validation and functional development of battery management for mobility applications.

Keywords: equivalent circuit model; extended Kalman filter; air-cooled battery thermal management system; model-based design of Li-ion batteries; online battery parameter estimation



Citation: Sophy-Mahfoudi, N.; Sekharam, S.-V.; Boutaous, M.; Xin, S. Model-Based Design of LFP Battery Thermal Management System for EV Application. *Batteries* **2024**, *10*, 329. <https://doi.org/10.3390/batteries10090329>

Academic Editor: Vilas Pol

Received: 29 June 2024

Revised: 12 August 2024

Accepted: 31 August 2024

Published: 18 September 2024



Copyright: © 2024 by the authors. Licensee MDPI, Basel, Switzerland. This article is an open access article distributed under the terms and conditions of the Creative Commons Attribution (CC BY) license (<https://creativecommons.org/licenses/by/4.0/>).

1. Introduction

The convergence of advancements in lithium-ion battery technology, battery management systems (BMSs) and thermal management solutions represents a paradigm shift in sustainable transportation [1]. As electric vehicles (EVs) continue to gain traction, optimizing battery performance, safety and longevity will remain at the forefront of research and innovation. Advanced numerical modeling techniques for modeling the battery parameters and developing battery management algorithms hold great promise for greener, cleaner and more efficient future mobility solutions.

In the realm of sustainable transportation and energy conservation, the advancement of EV technologies is fundamental to reduce the environmental impact and dependency on fossil fuels. Among the critical components of EV operation and efficiency, lithium-ion batteries (LiBs) stand out due to their unparalleled performance characteristics. They are valued for their high energy density, long service life and excellent energy efficiency. To realize the full potential of LiBs, advanced BMSs are essential [2]. These systems act as the nerve center of lithium-ion battery packs, ensuring safe and efficient operation while optimizing performance for a longer service life.

However, the thermal management of LiBs poses a significant challenge, especially in EVs. An efficient battery thermal management system (BTMS) is required for ensuring the longevity of LiBs by optimizing the operating temperatures and reducing the risk of thermal runaway [3]. BTMSs maintain battery operation within safe limits, extending battery life and improving the overall safety of the vehicle [4].

Among the various BTMS solutions, air-based systems have attracted widespread attention due to their adaptability and reliability [5]. Air-cooled BTMSs offer an attractive proposition for EV manufacturers seeking to balance performance, efficiency and safety. Understanding the thermal behavior of LiBs is critical to ensure their performance and safety [6]. While experimental approaches provide insight into battery operation, they are often limited by time, effort and accessibility limitations. In contrast, numerical simulations offer a versatile and flexible means to comprehensively investigate battery operation under a variety of conditions for design optimization and performance enhancement [7]. These simulations also allow for validation using different verification protocols like SIL, MIL and HIL for industrial production.

Among the different types of numerical characterization techniques for battery modeling, equivalent circuit models (ECMs) stand out as essential tools for understanding and modeling the non-linear electro-thermal behavior of LiBs [8]. ECMs simplify complex electrochemical processes within batteries, making it easier to accurately estimate critical battery parameters [9]. These models provide a structured framework for analyzing battery dynamics and optimizing automotive BMS accordingly.

The state of charge (SOC) is a critical parameter for battery management, and other battery parameters, such as the state of health (SOH), state of power (SOP) and state of energy (SOE), are essential for optimizing cell performance and ensuring the reliability of the battery pack [10]. However, the non-linear and time-varying characteristics of batteries pose significant challenges in developing battery parameter estimation algorithms [11]. Traditional methods, such as Coulomb counting, are often limited by error accumulation and initial charge deviation [12].

In contrast, real-time modeling techniques, such as the family of Kalman filters, and advanced technologies with the assistance of artificial intelligence (AI) like neural networks provide a robust solution for online SOC estimation and improve system accuracy for better cell performance [13].

Studies have demonstrated that equivalent circuit models (ECMs) improve the estimation of both the state of charge (SOC) and state of health (SOH), especially when combined with sophisticated estimation algorithms. For example, research has shown that integrating ECMs with machine-learning techniques, such as support vector machines (SVMs) [14] and neural networks [15], can substantially boost the accuracy of SOC estimation, particularly under constant current (CC) and constant voltage (CV) charging regimes.

In BMS, the integration of machine-learning algorithms and advanced model-based estimation techniques has significantly improved the accuracy of SOC and SOH estimation. Predictive thermal management algorithms are currently being developed to proactively predict thermal issues and adapt cooling strategies accordingly. These advances support ongoing efforts to improve the efficiency, safety and reliability of EV batteries to increase the adoption of electric vehicles. However, AI models can strain the currently available chip resources and require large amounts of data for training, making Kalman filters a more practical choice for real-time vehicle applications [16,17].

Accurately determining battery parameters is crucial for implementing the designed models, particularly on functional frameworks like embedded devices to perform the desired tasks by the BMS [18]. The functional development of BMS algorithms for real-time application can be achievable by using ECMs and online estimation algorithms like extended Kalman filters for accurate prediction of battery parameters [19].

This paper details the ECM of LiFePO₄ batteries and the method used for the extraction of battery parameters from HPPC test data for model-based design. It also covers the implementation of the SOC estimation algorithm using the extended Kalman filter for online parameter identification and functional development of BTMS, including air cooling. The developed model estimates battery parameters as a function of the applied load and provides insight into key metrics, such as the state of charge (SOC) and state of health (SOH).

The real-time test data used in this paper highlight the current importance of such data and provide valuable insights for validating model-based designs for Li-ion batteries

and BMS. The paper concludes with an overview of the results and a discussion of the challenges in SOC estimation using the extended Kalman filter, thoroughly investigating the topic from inception to completion and beyond.

2. Single-Cell Characterization

2.1. Experimental Setup

The battery test bench used to characterize the cell is visualized as follows (in Figure 1):

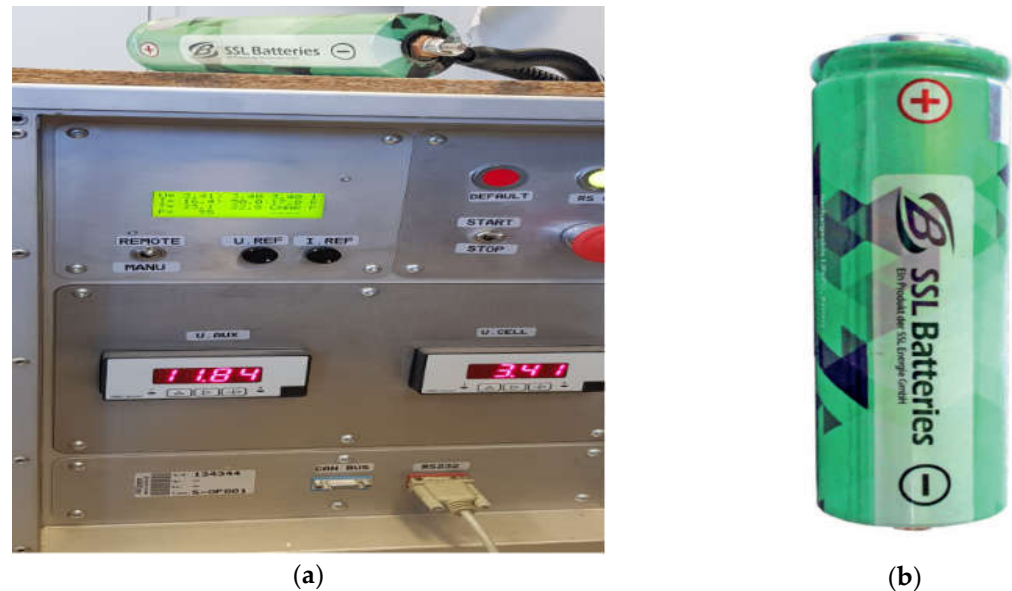


Figure 1. Cell characterization test bench: (a) Cell testing equipment; (b) SSL battery.

The SOC–OCV relationship obtained from the test bench is represented in Figure 2.

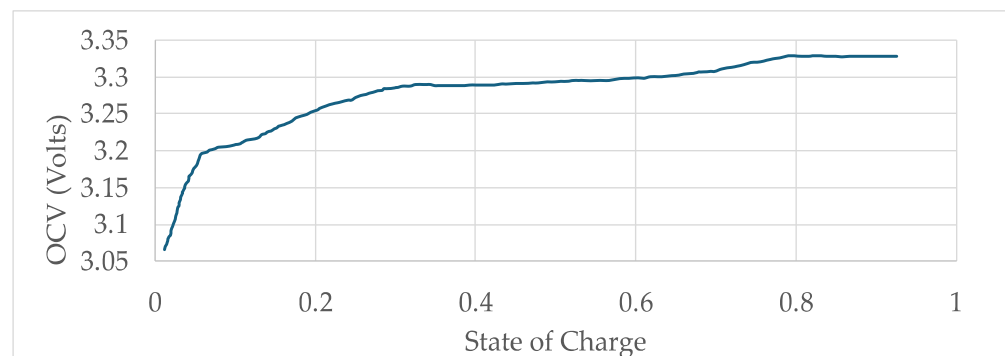


Figure 2. OCV vs. SOC profile of SSL battery.

For the purpose of cell characterization, a hybrid pulse power characterization (HPPC) test is performed to evaluate the battery response. The HPPC test provides critical data for battery management systems, aiding in the development of batteries.

The setup involves fully charging the battery, connecting it to a battery tester for precise current control and using a thermostatic chamber to stabilize the battery temperature if necessary. The test procedure involves applying short, high current discharge and charge pulses at various states of charge (SOC).

Typically, the test starts at 100% SOC and gradually decreases, e.g., by 10%, until a predefined lower limit is reached. During each pulse, the voltage and current data are recorded to calculate the internal resistance of the cell.

The current profile used in the HPPC test are visualized in Figure 3, providing insight into the dynamic behavior of the cell.

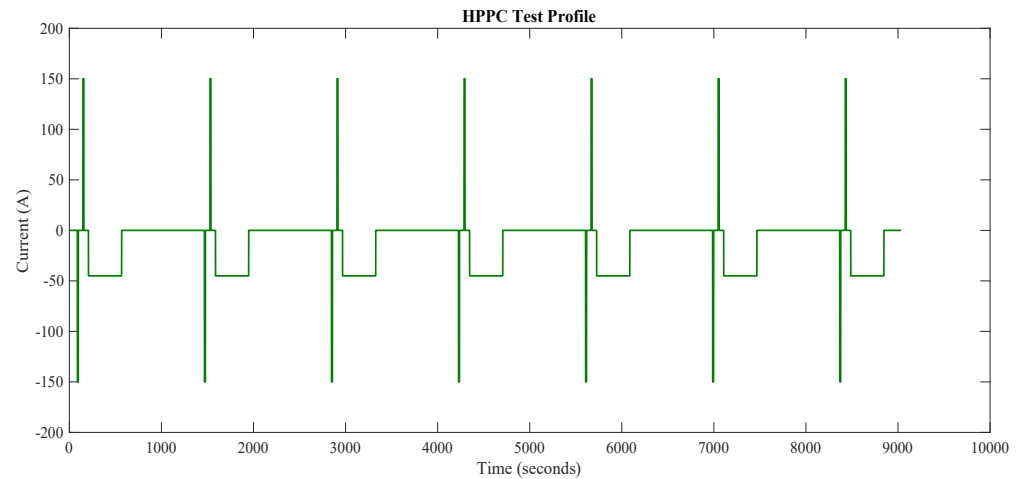


Figure 3. HPPC current profile.

The terminal voltage of the test cell measured on the test bench during the HPPC test used for the estimation of cell parameters is visualized in Figure 4.

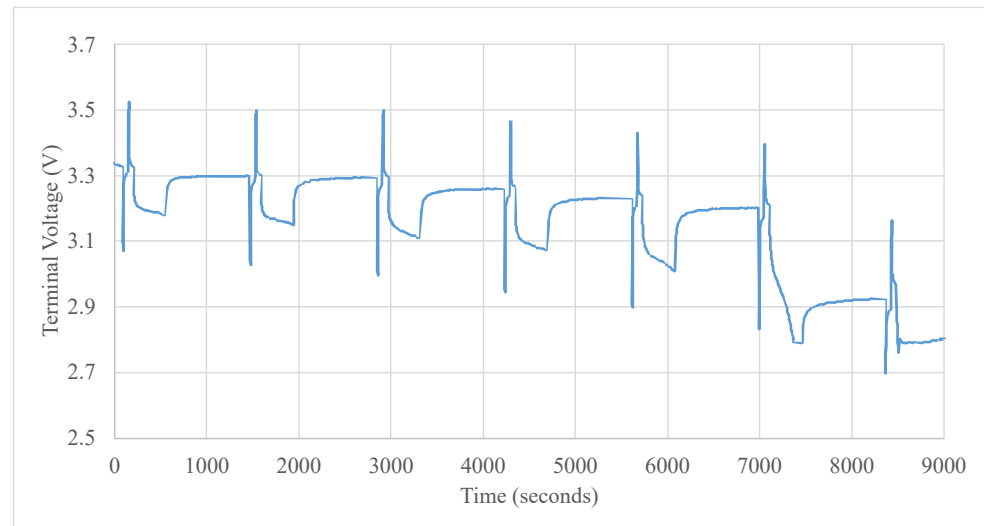


Figure 4. HPPC cell characterization data.

2.2. Electrical Modeling of the Cell

To improve the accuracy of the battery state of charge (SOC) estimation, it is important to develop an equivalent circuit model (ECM) that not only provides high accuracy but also faithfully represents the dynamic characteristics of the battery.

A second-order Thevenin model with two RC networks is chosen for a comprehensive representation of the electrical behavior. These networks are crucial for simulating both short-term transients and long-term behavior.

The second-order Thevenin model is extended to include a variable voltage source to model the open circuit voltage of the cell, a series-connected variable resistor for ohmic resistance and two parallel RC branches with variable resistors and capacitors to model the polarization and charging and lowering transfer voltages as a robust foundation.

The obtained cell characterization data in Figure 4 effectively represent the transient response and steady-state characteristics of a Li-ion battery, which are denoted by

$$\tau_1 = R_1 \times C_1, \quad (1)$$

$$\tau_2 = R_2 \times C_2 \quad (2)$$

Figure 5 illustrates the construction of the ECM, showing components such as variable capacitors, resistors and controlled voltage sources.

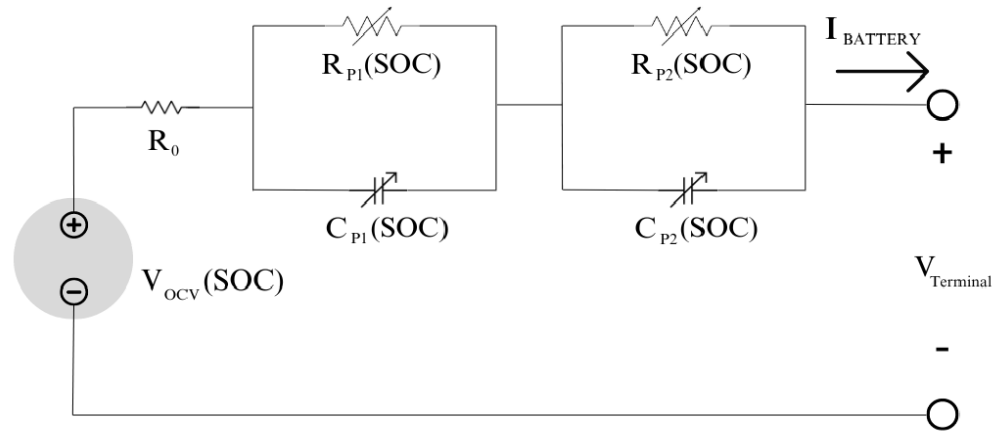


Figure 5. Schematic of the second-order Thevenin model.

These elements combine to simulate important aspects, such as cell capacity and SOC dynamics; key to the accuracy of the model is the voltage-controlled voltage source, which non-linearly relates the SOC to open circuit voltage (OCV). The resistors R_0 , R_1 and R_2 each represent a different physical process in the cell.

R_0 or series resistance: It represents the total ohmic resistance in the circuit, including the effects from the electrolyte, current collectors and contact resistance at the interfaces, which affect the cell’s initial response to an applied voltage or current. Higher R_0 values can lead to increased energy losses during operation.

R_1 : It corresponds to the charge transfer resistance at the electrode interface during the charge and discharge process and significantly affects the kinetics of lithium-ion insertion and desorption. Lower R_1 values indicate more favorable kinetics, leading to better battery performance, especially at higher temperatures and speed cycling.

R_2 : It refers to the resistance encountered by lithium-ions as they diffuse through the solid electrode material. This is especially important for mass transport at higher states of charge or faster cycling.

Analyzing these resistance components can provide researchers with insight into the electrochemical behavior of lithium-ion batteries and allow targeted refinements of materials and designs to improve performance.

In this paper, we consider all the ECMs to be a function of SOC; thus, the terminal voltage of the cell is represented as follows:

$$V(t) = OCV - V_{ohmic} - V_{RC1} - V_{RC2} \tag{3}$$

For the two R–C pairs, the voltage observed at the terminals is governed by

$$V(t) = I(t) \times R_{ohmic} + \tau_1 \frac{dV_{c1}}{dt} + \tau_2 \frac{dV_{c2}}{dt} \tag{4}$$

where $V(t)$ is the terminal voltage over time; $I(t)$ is the load current; R_{ohmic} is the ohmic resistance of the cell; and V_{c_n} are the capacitor voltages.

2.2.1. Identification of Cell Parameters

A regression algorithm referenced from [20] was developed to identify the voltage drops at the current profile of 1C rate, and Figure 6 represents the windows, which are referenced in the algorithm to develop the cell parameters from cell characterization data.

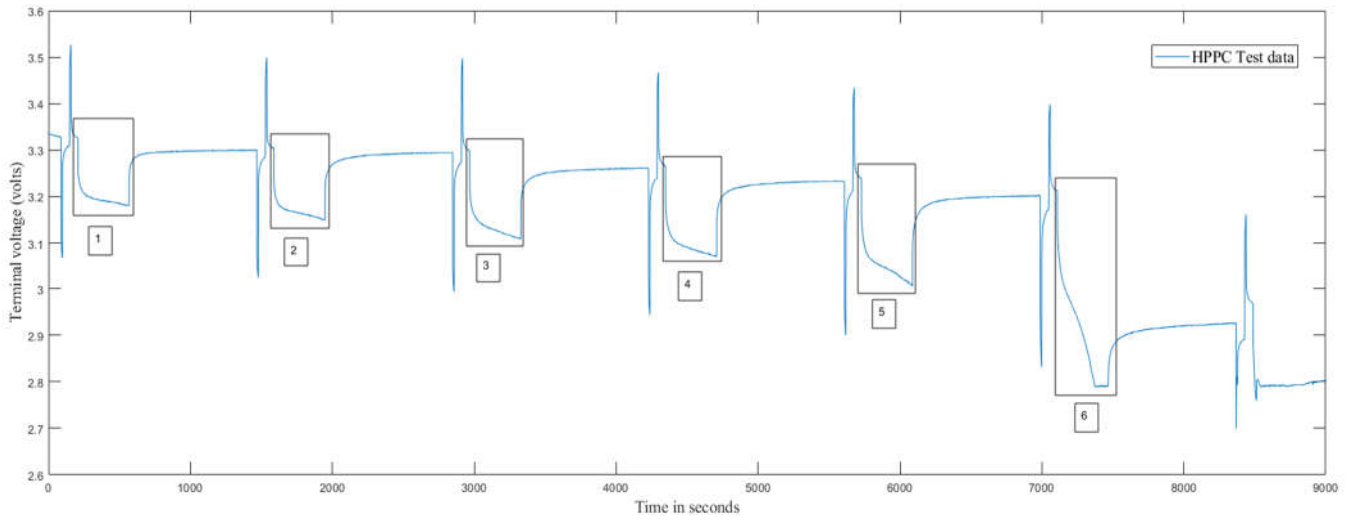


Figure 6. Referencing of specific pulses in cell characterization data by the algorithm.

To identify the different parameters of the cell for modeling a 2RC Thevenin model, the data obtained from the cell characterization test are used. These data contain the battery profile in the form of pulses at each respective square load profile. The characterization consists of several key components:

1. Instantaneous voltage drop (V_0 to V_1): This drop is due to the ohmic resistance of the connectors, electrodes and electrolyte (R_0).
2. First voltage drop (V_1 to V_2): This represents the mass transport effects within the cell.
3. Second voltage drop (V_2 to V_3): This reflects the double-layer effects during each discharge pulse.

The following voltage drops characterized on the discharge pulse at the respective SOC for estimating cell parameters are shown in the Figure 7.

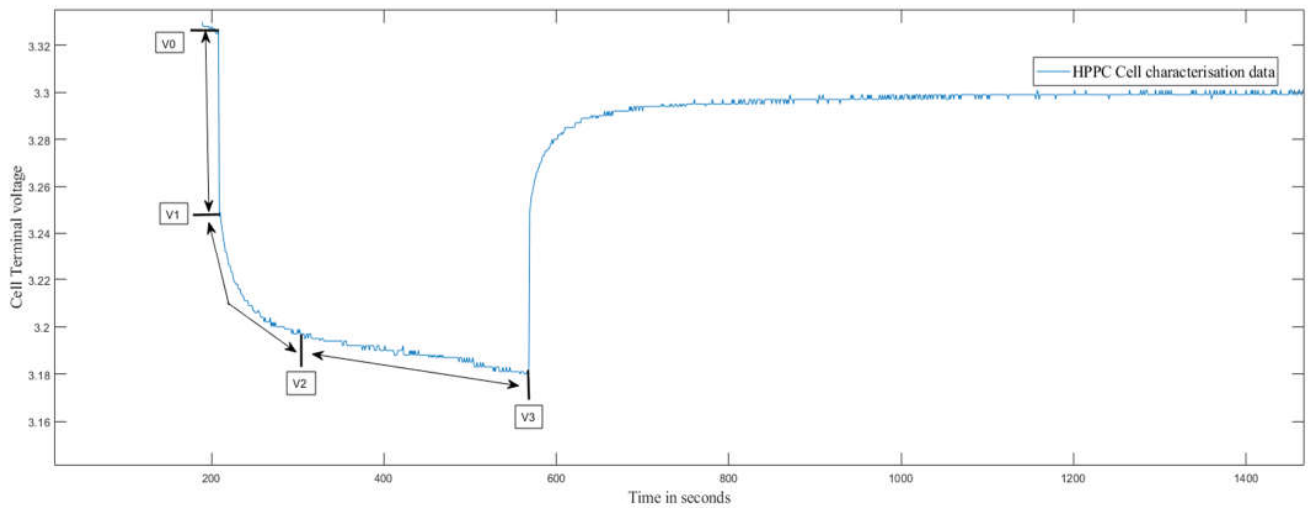


Figure 7. 2RC ECM parameter estimation.

Parameters such as V_0 , V_1 , V_2 , V_3 , τ_1 , τ_2 serve as the regression parameters. Then, the parameters of the battery equivalent circuit model, which are OCV, R_0 , R_1 , R_2 , C_1 , C_2 , can be defined as follows:

$$R_0 = \frac{V_0 - V_1}{I} \tag{5}$$

$$R_1 = \frac{V_1 - V_2}{I} \tag{6}$$

$$R_2 = \frac{v_2 - v_3}{I} \tag{7}$$

The obtained R_0 , R_1 , R_2 are used in the calculation of c_1 and c_2 from Equations (1) and (2).

For all the different time segments of different SOC values at each HPPC current profile, through parameter identification, the equivalent circuit model parameters are obtained, and the obtained parameter values from HPPC test data are visualized in Figure 8.

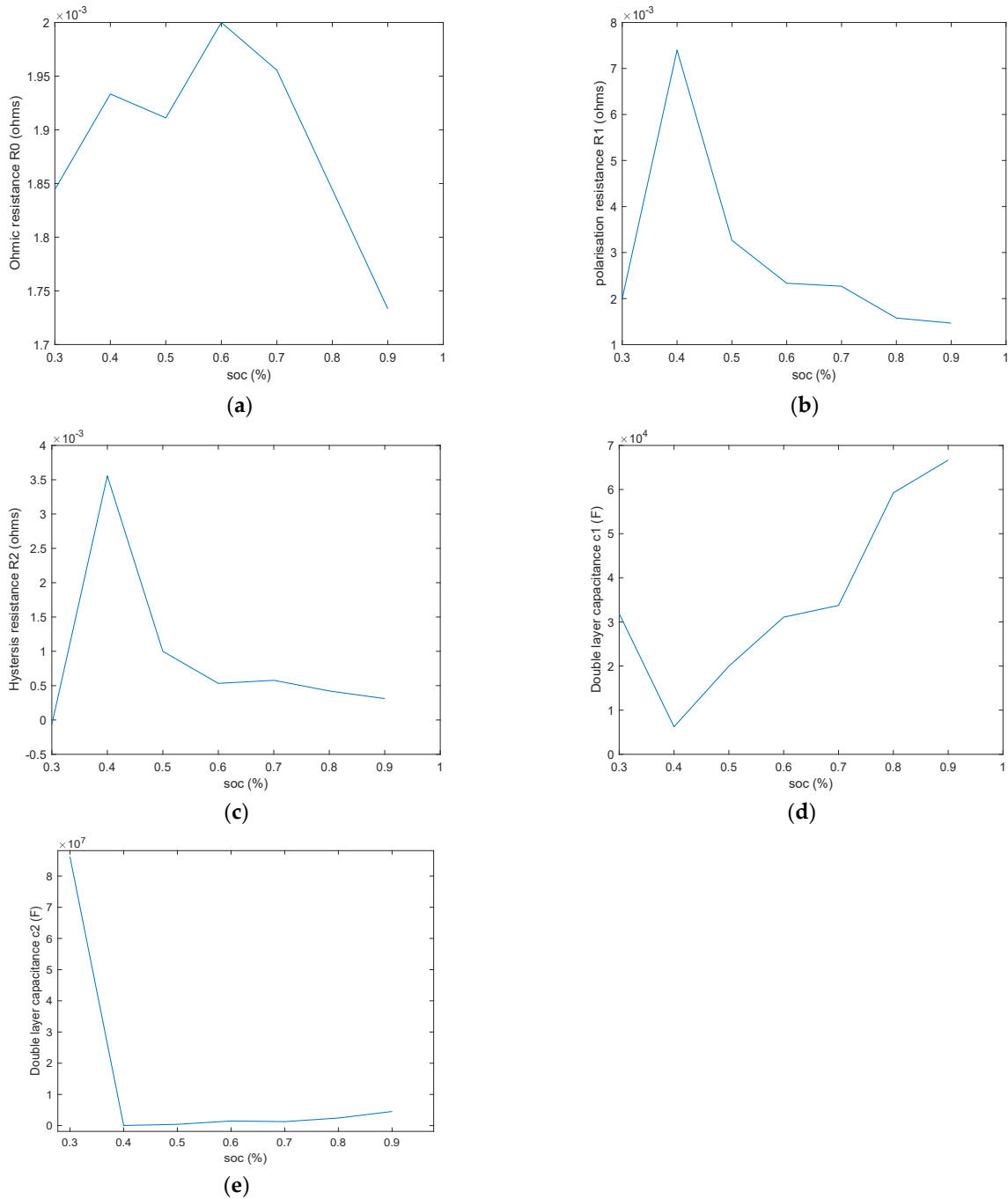


Figure 8. (a) Represents the values of ohmic resistance R_0 with SOC; (b) represents the values of polarization resistance R_1 with SOC; (c) represents the values of hysteresis resistance R_2 with SOC; (d) represents the values of double-layer capacitance C_1 with SOC; (e) represents the values of double-layer capacitance C_2 with SOC.

2.2.2. Validation of the Cell Model

The single-cell model was validated using Coulomb counting for the state of charge (SOC) estimation applied to a 2RC Thevenin circuit. The equivalent circuit model (ECM) parameters of the cell were modeled as a function of SOC and temperature. The current profile used for cell characterization was also used to validate the model by simulating it with voltage measurements taken from a test device.

The parameters of the simulated battery are listed in Table 1.

Table 1. Parameters of LFP Li-ion SSL battery.

Quantity	Parameter	Unit
Cell chemistry	LFP (Lithium iron phosphate)	-
Battery rated capacity	45	Ah
Battery rated voltage	3.3	V
Charging cut-off voltage	3.65	V
Discharge voltage	2.8	V
Specific energy	148	Wh
Max. continuous discharge	<50	A
Recommended charging current	Up to 45	A

The validation results indicate the ECM modeled with estimated battery parameters in Figure 9. However, there are deviations in accurate prediction of the cell voltage, with RMSE and MAE errors reaching up to 0.4% at certain instances. These deviations suggest that further refinement of parameter estimation using advanced numerical methods is necessary to improve the model's accuracy for implementation in real-time applications.

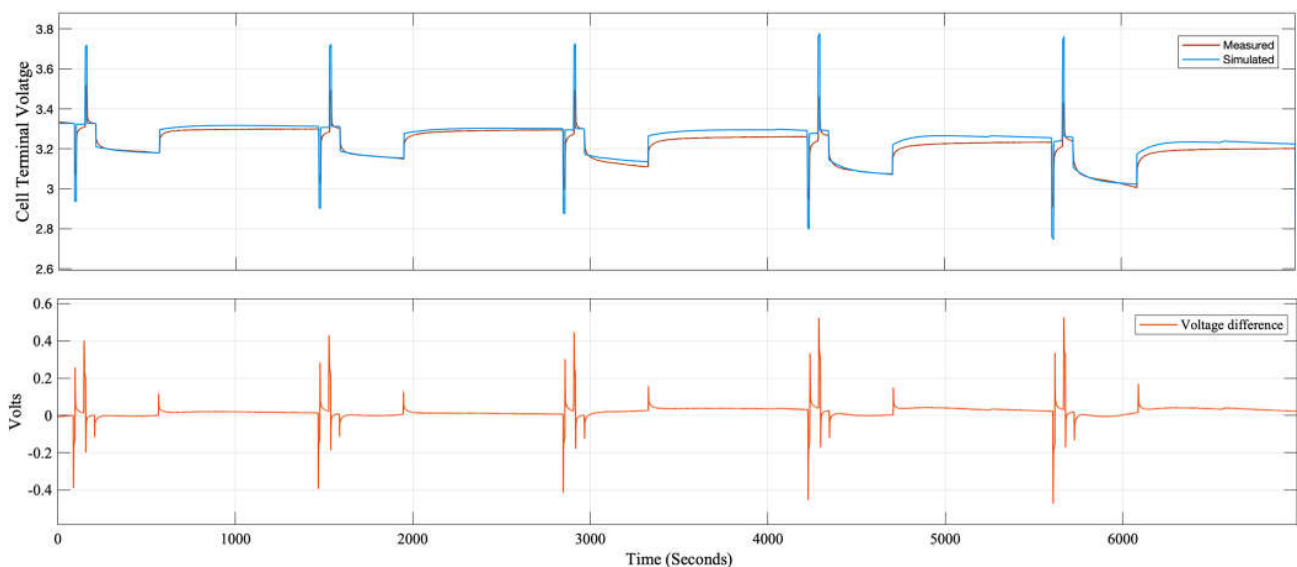


Figure 9. ECM model validation results.

3. Thermal Modeling

Battery thermal management and electrical operation are closely linked, as battery performance and safety are significantly affected by temperature. During charge and discharge cycles, batteries generate heat due to internal resistance and electrochemical reactions, which in turn affect the battery's temperature.

These temperature variations affect the battery's electrical performance, including capacity, efficiency and internal resistance. High temperatures can increase capacity loss, while low temperatures can reduce the available capacity and increase internal resistance. Furthermore, excessive heat can cause thermal runaway, a hazardous condition that can

result in fires and explosions, highlighting the need for effective thermal management to prevent such incidents.

Maintaining the cells within a specific temperature range ensures maximum performance and lifespan. Heat generation in the cell occurs primarily through an irreversible process due to the internal resistance while the current is flowing, and it is defined as follows:

$$Q_{\text{irreversible}} = I^2 \times R \times t \quad (8)$$

where $Q_{\text{irreversible}}$ (Joules) is the rate of irreversible heat generation; I (Amperes) is the current flowing through the cell; R (Ohms) is the cell's internal resistance; t (seconds) is the time during which the current flows.

The fundamental principle of heat transfer under steady-state conditions governing the thermal behavior of the cell is defined as follows:

$$Q_{\text{irreversible}} = Q_{\text{conduction}} + Q_{\text{convection}} + Q_{\text{radiation}} \quad (9)$$

where $Q_{\text{conduction}}$ (Joules) is the rate of heat transfer through conduction; $Q_{\text{convection}}$ (Joules) is the rate of heat transfer through convection; $Q_{\text{radiation}}$ (Joules) is the rate of heat transfer through radiation.

As our approach is a lump-based model, the $Q_{\text{conduction}}$ is neglected, and the temperature range remains at a low temperature range; thus, $Q_{\text{radiation}}$ is neglected. Only convective heat transfer ($Q_{\text{convection}}$) is considered in this paper.

$$Q_{\text{convection}} = h \times A \times (T_{\text{cell}} - T_{\text{ambient}}) \quad (10)$$

where h (W/m^2K) is the convective heat transfer coefficient; A (m^2) is the surface area of the cell; T_{cell} (K) is the cell temperature; and T_{ambient} (K) is the ambient temperature.

4. State of Charge Prediction

The state of charge (SOC) reflects the remaining capacity of the battery relative to its maximum capacity and is essential for monitoring battery health, predicting runtime and optimizing power management strategies.

4.1. Coulomb Counting

For a LiB, during the discharge or charge process, its SOC using Coulomb counting can be defined as follows:

$$\text{SOC}(t) = \text{SOC}(t_0) - (1/Q) \int_0^t i(\tau) d\tau \quad (11)$$

where $\text{SOC}(t_0)$ is the SOC of Li-ion battery at moment t_0 ; $i(\tau)$ is the current flowing through the battery at moment τ ; and Q is the rated capacity of the battery.

This approach, however, is very sensitive to measurement errors, as visualized in Figure 9. In addition, the Coulomb counting algorithm requires the correct initialization with the initial SOC value, which may not be available, as occurs in HEVs, where the battery is never fully charged or discharged.

When operating a battery, random noise in the observations of current, voltage and other physical quantities can lead to the accumulation of errors when calculating the state of charge (SOC) using the Ah method. Over time, this leads to a decrease in the accuracy of the estimation. To solve this non-linear estimation problem, the "extended Kalman filter" (EKF) algorithm is used.

4.2. Extended Kalman Filter for Online Estimation of Battery Parameters

The EKF is an optimal autoregressive data processing algorithm that achieves minimum variance estimates through a recursive approach, providing both the estimate and the associated error. The discrete non-linear state-space model of the EKF is particularly well

suitable for this application [21], allowing for accurate and reliable SOC estimation despite the presence of observation noise and inherent non-linearities in battery operation.

As the Kalman filter requires a cell model, the discrete non-linear state-space representation reference used for this purpose is shown below:

$$\begin{cases} X_k = f(X_{k-1}, U_{k-1}, w_{k-1}) \\ Y_k = h(X_k, U_k, v_k) \end{cases} \quad (12)$$

$$w_k \sim (0, Q) \quad (13)$$

$$v_k \sim (0, R) \quad (14)$$

where w_{k-1} is the process noise value at moment $k-1$; v_k is the measurement noise value of moment k ; Q is the covariance of w_k ; R is the covariance of v_k .

4.2.1. Linearization of Charge Utilized

The EKF approximates these non-linear functions using a first-order Taylor expansion around the current estimate. This process involves computing the Jacobian matrices of the state transition and measurement functions. These Jacobians are used to linearize the non-linear model around the current state estimate.

The OCV_SOC profile obtained from cell characterization data, which is represented in Figure 2, is converted into a polynomial equation representing the open circuit voltage as a function of SOC and then differentiated by first order to form a polynomial equation representing the charge utilized as a function of the state of charge.

$$C_u = P_7 * SOC_{predict}^6 + P_6 * SOC_{predict}^5 + P_5 * SOC_{predict}^4 + P_4 * SOC_{predict}^3 + P_3 * SOC_{predict}^2 + P_2 * SOC_{predict}^1 + P_1 \quad (15)$$

The state of charge predicted by the EKF algorithm is utilized to calculate the output. The main idea of the EKF is to use the state equations to predict the state variables of the system at the next instant in time. By linearizing the non-linear battery model, the EKF can effectively handle the inherent non-linearities and provide more accurate and reliable SOC estimates.

4.2.2. State-Space Matrices

An equivalent circuit model with state-space matrices is established as follows:

$$A = \begin{bmatrix} 0 & 0 & 0 \\ 0 & -1/\tau_1 & 0 \\ 0 & 0 & -1/\tau_2 \end{bmatrix}, \quad B = \begin{bmatrix} (-\text{eff} * \Delta T)/Q \\ R1 * (1 - e^{(-\frac{\Delta T}{\tau_1})}) \\ R2 * (1 - e^{(-\frac{\Delta T}{\tau_2})}) \end{bmatrix}, \quad C = \begin{bmatrix} C_u \\ -1 \\ 1 \end{bmatrix} \quad (16)$$

The states and parameters comprise fast and slow dynamics of the battery. Specifically, there is a difference in the model-predicted terminal voltage value applied to the load. Also, the real-time measured voltage value of the cell is used to calculate the error or minimum variance estimate to update the Kalman gain coefficients accordingly, which are used to modify the weights of the observations and predictions when computing the estimates of the state variables, and the steps involved in the process of an extended Kalman filter are presented in the below Table 2.

The P_k is the error covariance, and the K_k is the Kalman gain coefficient. In each sampling cycle, the EKF algorithm must estimate the P_k and X_k in two different ways, including priori estimation and posteriori estimation. Between the two stages, the Kalman gain coefficient K_k is calculated by the priori estimate.

This representation expresses the system's behavior using matrices in Equation (16) and differential equations, relating its state variables, inputs (load current, U_k) and outputs (load voltage, Y_k and soc_k).

The Kalman filter is initialized with a priori state estimates when the vehicle is turned on (based on OCV readings and the prior SOC when the vehicle was turned off). The

algorithm then repeatedly updates the state estimate and state-uncertainty (error bound) estimate with each set of new measurements as the system runs. The results are presented based on a real-time test in the results section; they show that accurate SOC estimation with very tight error bounds is obtained whether the initial SOC estimate is accurate or not.

Table 2. Details of the process inside the EKF algorithm.

Steps	Process
Step 1	Initial state variables, x_0, y_0
Step 2	Covariance matrix, P_{k-1}
Step 3	Predicted states, $X_k = A_{K-1} * X_{k-1} + B_{K-1} * U_{K-1} + Q_{K-1}$
Step 4	Predicted error covariance matrix, $P_k = A * P_{k-1} * A^T + I * Q$
Step 5	Calculation of the error value between the predicted and the measured states
Step 6	Calculation of Kalman gain, $K_k = (P1 * C^T) / (C * P * C^T + R)$
Step 7	State estimation measurement update, $X_{K+1} = A_{K+1} + K (Y_{K+1} - X_{K+1})$
Step 8	Error covariance measurement update, $P_{k+1} = (I - K * C) * P_k$

Using the measurement equation, the Kalman filter calculates the generalized errors between the measurable value and the system dynamic variables (including the SOC). Then, the Kalman gain is used to update the estimation values of the state variables.

The estimation approach depicted in below Figure 10 reveals that a single EKF is sufficient for simultaneous online battery parameter estimation. The figure likewise demonstrates how the information flows from one step to another during estimation.

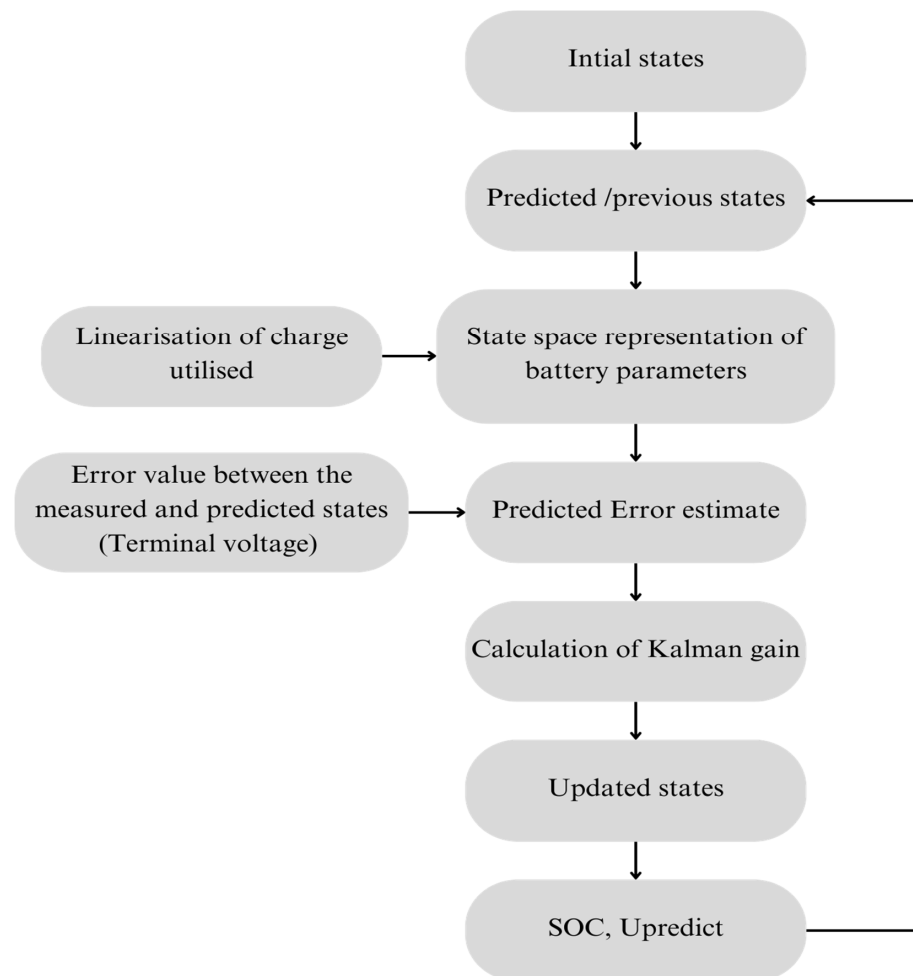


Figure 10. Detailed structure of the EKF for estimation of battery parameters.

5. State of Health Estimation Using Impedance Tracking and Coulomb Counting

Accurate estimation of the battery’s state of health (SOH) is critical to ensure reliable performance and lifespan. SOH estimation techniques provide insight into the remaining useful life of a battery and help in maintenance planning and preventing unexpected failures [22]. Among the various methods available, impedance tracking and Coulomb counting stand out due to their effectiveness and complementarity.

The SOH of the cell is calculated by considering the charge at the start, that is, Q_{start} the charge utilized by the load, that is, ΔQ ; and the charge remaining in the cell at the end of discharge, which give us the estimation of nominal capacity of the cell, as visualized in below Figure 11.

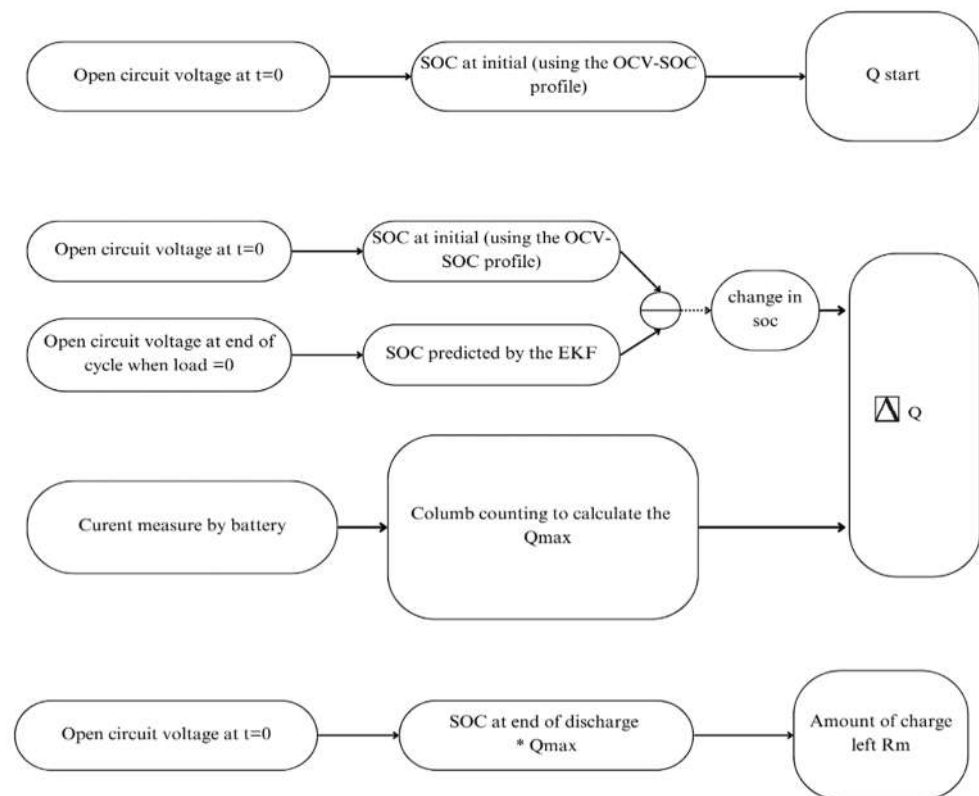


Figure 11. Schematic of SOH estimation process using coulomb counting method.

The acquired nominal capacity of the cell can be compared with the nominal capacity of the cell in the fresh condition using the following equation:

$$SOH = (Q_{measured} / Q_{nominal}) \times 100\% \tag{17}$$

6. Design of BTMS

In terms of battery thermal management, keeping batteries within acceptable temperature ranges is critical for their performance, durability and general safety. One extensively used approach is air cooling, which uses fans to remove the heat generated during battery operation. This introduction will explain the notion of air-cooling systems that use two fans over a battery pack with 12 cells. Furthermore, it will investigate the integration of an automated control system to govern the operation of these fans, guaranteeing effective cooling while minimizing energy usage [23,24].

6.1. Fan Control Algorithm

The fan control algorithm for battery cooling was created using Simulink State flow and Design flow chart is visualized in below Figure 12. This graphical environment

provides a visual depiction of the control logic, making it easier to comprehend and alter. The design method entailed designing four states: Manual On, Manual Off, Auto On and Auto Off. The transitions between the states were created using human input and temperature sensor data from important spots throughout the battery pack. The Auto On mode operates the cooling fan when temperatures surpass a predetermined higher limit, while the Auto Off state deactivates the fan when temperatures fall below a lower limit.

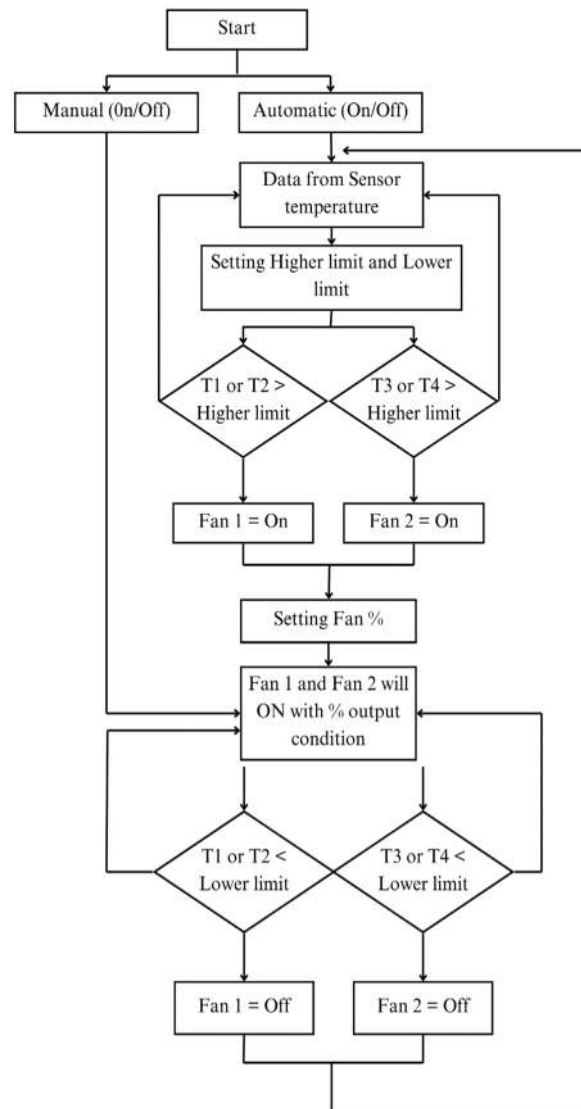


Figure 12. Fan control algorithm.

User input allows the user to override the automated control and manually switch the fan on or off. State flow actions were used to regulate the “fan control signal” transmitted to the actual cooling fan, allowing for variable fan speed control via duty cycle modifications. This design enables optimal thermal management of the battery by automatically controlling the cooling fan based on temperature conditions while still allowing for user intervention when needed.

6.2. Integration of BTMS with EKF for Online Estimation of Battery Parameters

The model-based design, originally presented in [14], provides a framework for estimating the state of charge (SOC) in a battery management system (BMS).

In our approach, the measured current (I_{cell}) is integrated with an extended Kalman filter (EKF) to achieve real-time estimation of the state of charge (SOC). The EKF-based SOC

estimation is coupled with a cell equivalent circuit model (ECM) that is carefully developed using detailed cell characteristic data.

The EKF works by estimating the voltage drop between the RC circuit and the SOC using a state-space representation matrix. SOC is fed back to the ECM closed circuit to predict the cell terminal voltage. In this closed-circuit system, the measured voltage serves as the reference input. The difference between the actual and predicted voltages is calculated and used in the update step of the EKF to predict the state for the next time interval.

In our model-based BMS design, the EKF effectively addresses the limitations of traditional Coulomb counting methods by accounting for observation noise and non-linearities. It also leverages a discrete non-linear state-space model of the cell and iteratively minimizes the variance in the SOC estimate using a recursive algorithm.

This robust methodology ensures accurate and reliable SOC estimation, which is critical for an efficient battery management strategy. To validate the performance of the EKF-based model, a comparison is performed with the SOC estimates obtained using the Coulomb counting method, which demonstrates good robustness and accuracy in real applications.

The layout shows the overview of a battery management system (BMS) designed using air-cooled Li-ion battery pack in a 6S-1P configuration with online parameter estimation. The system starts with an external power demand input that the BMS needs to manage to ensure the safe operation of the battery pack.

The BMS handles tasks such as power monitoring, cell balancing and fan speed control while estimating the state of charge (SOC) using Coulomb counting. The battery pack receives a controlled current input from the BMS to ensure uniform charging and discharging of all cells.

The estimated SOC is compared with the actual SOC to determine the error, which is then processed by an extended Kalman filter (EKF). This EKF consists of a propagation step and a correction step to refine the SOC estimate and provide revised system state outputs. The designed model of BMS enables accurate real-time monitoring and management of the battery pack to ensure optimal performance and lifespan.

7. Simulation and Analysis

To investigate the effectiveness of the proposed method, a simulation model of the entire BMS was created in MATLAB/Simulink (2024 A), as described in the BMS layout in below Figure 13. The analysis begins with an examination of the cell terminal voltages and compares the real-time test data with the voltages simulated using the 2RC equivalent circuit model (ECM).

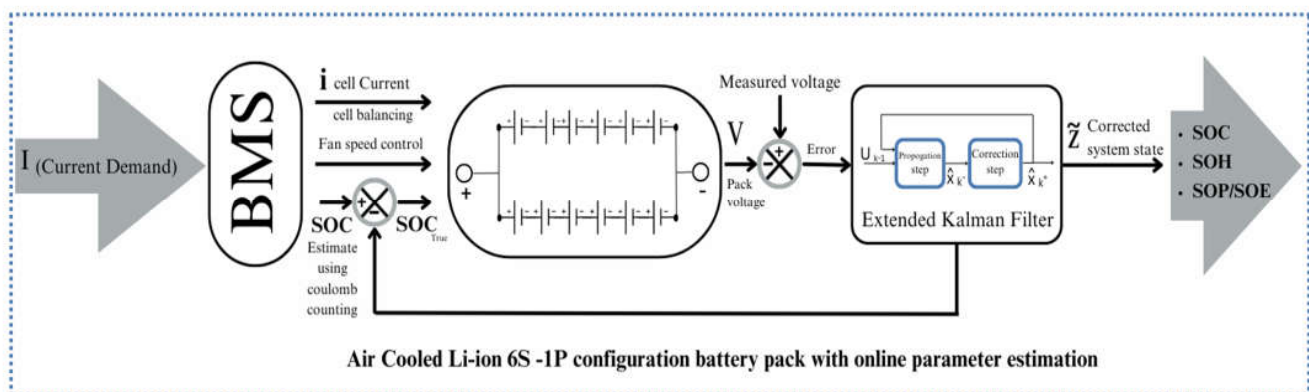


Figure 13. Layout of the model-based design of BTMS.

7.1. Voltage Predicted by the Model for HPPC Test

The performance of the cell voltage model was evaluated by comparing the predicted terminal voltage with the measured real-time voltage data during cell discharge.

Despite a higher initial error, the EKF algorithm effectively fine-tunes the battery parameters over time. As illustrated in Figure 14, the estimation error decreases progressively. Compared to the Ah method, which exhibits an error of 0.4%, the EKF achieves a significantly lower average estimation error of less than 0.1%. This demonstrates the superior accuracy and reliability of the EKF approach in estimating battery parameters.

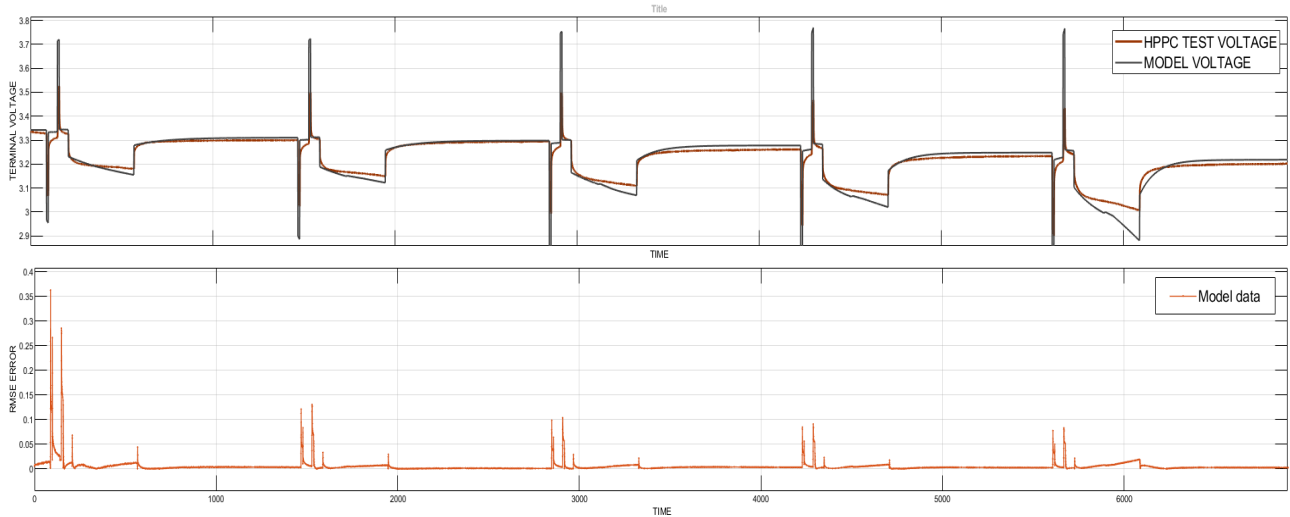


Figure 14. Cell voltage predicted by the EKF for the HPPC test profile.

7.2. Model Validation Using Real-Time Current Profile

The load profile was obtained from the electric vehicle tests carried out as part of the InnoTherms project and is visualized in Figure 15.

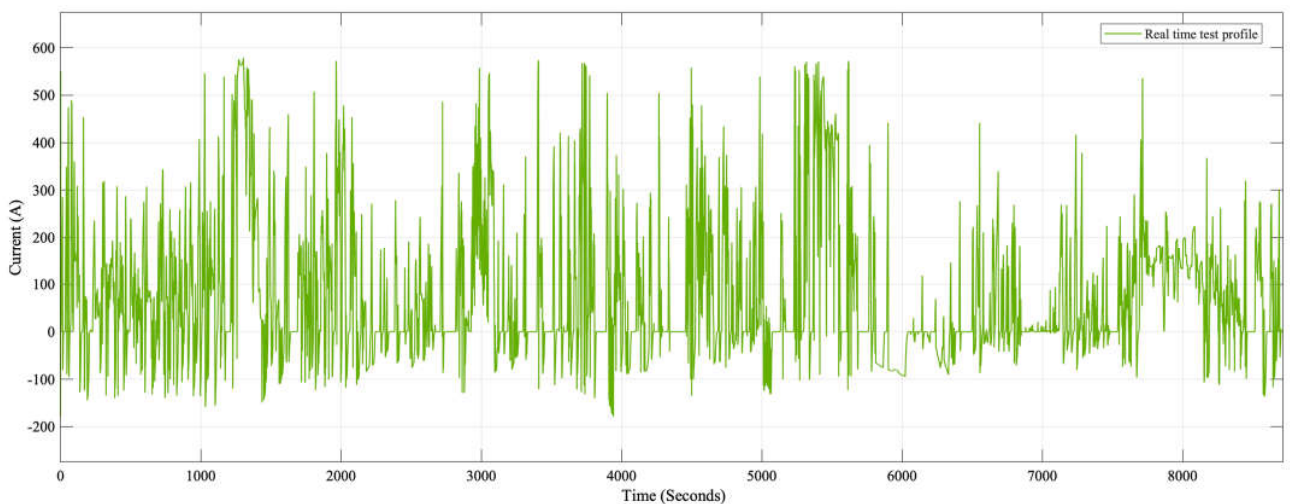


Figure 15. Real-time discharge profile.

The current measured at the battery was collected from the test vehicle operating under real-time conditions. These data are utilized to validate the battery management system (BMS) model and to predict battery parameters accurately.

The performance of the cell voltage model was evaluated by comparing the predicted terminal voltage with the voltage data measured in real time during the cell discharge, as visualized in Figure 16.

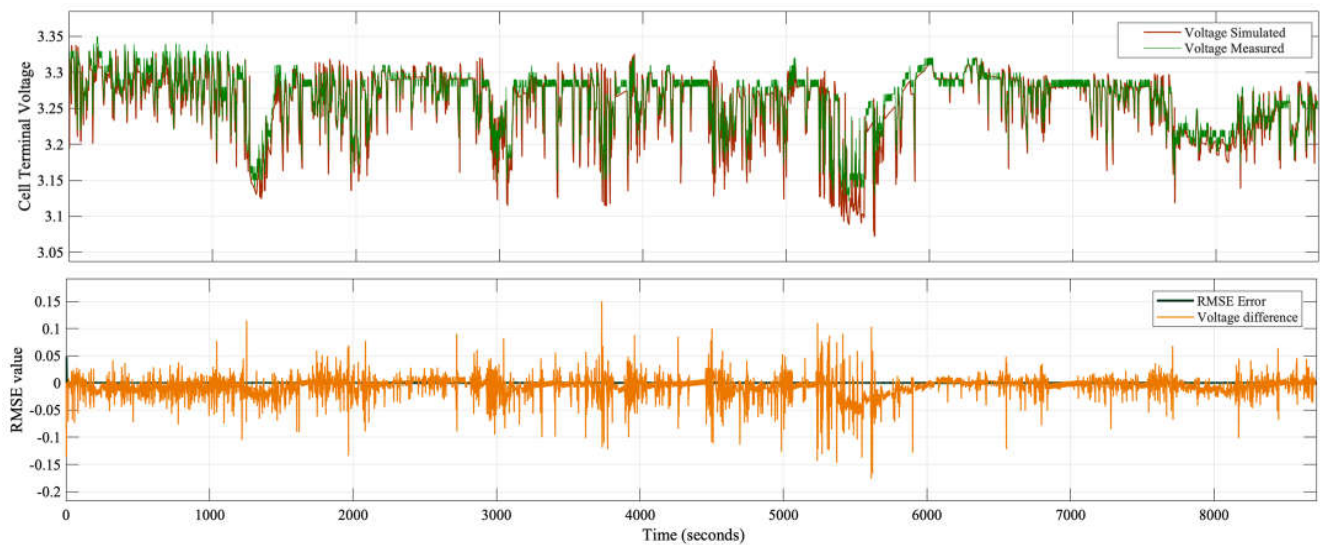


Figure 16. Cell terminal voltage and RMSE.

After experimentation with different sample times, fixed step sizes and model tolerances, the following results were obtained with a fixed step size and sample time of 0.15 and a model tolerance of 0.001. These settings showed that the model allows for accurate prediction of the battery parameters.

The close agreement between these two data sets over most of the experimental time frame indicates that the 2RC-ECM effectively captures the dynamic behavior of the cell's voltage response over the entire cycle. Although the root-mean-square error (RMSE) analysis highlights some discrepancies, the errors are still confined to a narrow range, indicating that the model is robust under dynamic loading conditions and effectively filters out noise.

Moreover, the minimal deviations observed in the error plots highlight the model's robustness in dealing with dynamic loading conditions and noise.

7.2.1. State of Charge Results

SOC predictions using the Coulomb counting (CC) method and the extended Kalman filter (EKF) algorithm are visualized in Figure 17.

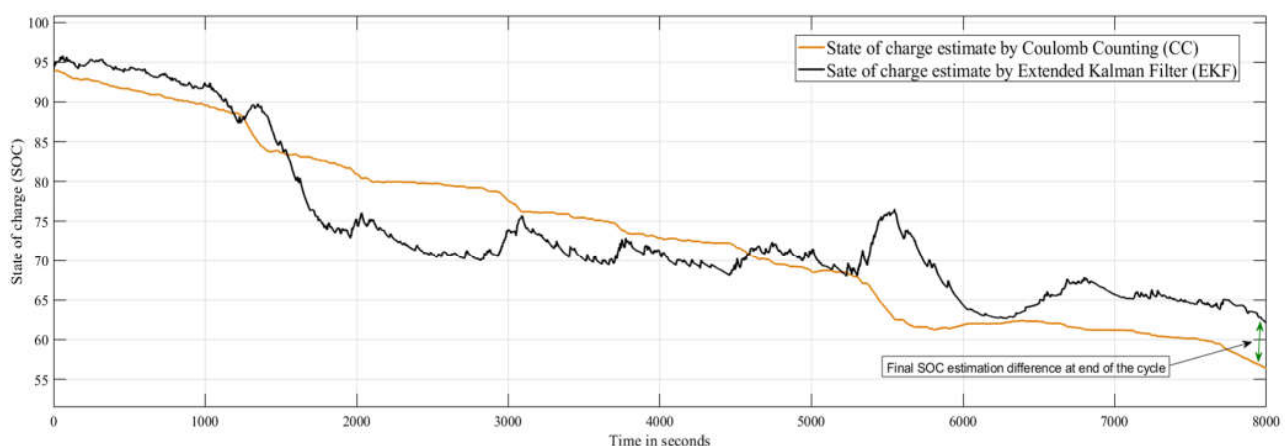


Figure 17. State of charge predictions.

Initially, the CC and EKF methods are close to each other. As the experiment progresses, the EKF's ability to incorporate new measurements and adjust its estimates accordingly becomes apparent, allowing for more accurate SOC tracking. This adaptability is critical

to managing the cumulative errors and inherent noise associated with real-time battery operation; the CC method has limitations in these areas. The deviation between the estimates of the two methods becomes larger, especially under high discharge and varying load conditions, highlighting the superior performance of the EKF in maintaining accuracy over time.

7.2.2. Visualization and Analysis of Temperature Prediction

The analysis typically involves plotting two key sets of data; the actual temperature measurements and the temperature predicted by the model is visualized in below Figure 18.

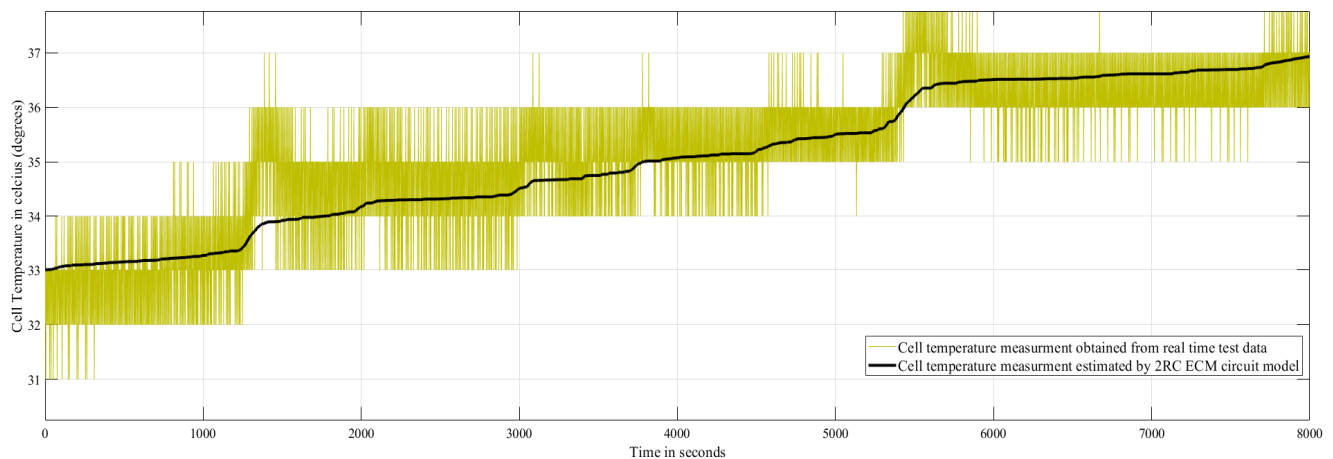


Figure 18. Model-predicted temperature with reference to measured temperature.

The optimal results in Figure 18 show high agreement between the real-time temperature data and the model predictions throughout the cycle. Such a close agreement means that the temperature model is robust and accurate, effectively capturing the thermal behaviors of the cell.

This validation not only improves the safety and efficiency of battery operations but also contributes to the broader goal of advancing battery technology for a variety of applications. Also, implementing an extended Kalman filter (EKF) for a state of charge (SOC) prediction by a battery management system (BMS) poses a number of complex challenges that require meticulous attention to ensure optimal performance.

8. Conclusions

A major advancement in the field of battery technology is made by integrating the equivalent circuit model (ECM) and an extended Kalman filter (EKF) into battery management systems (BMSs). This model-based approach not only captures the dynamic behaviors of the battery more accurately but also improves the accuracy of SOC prediction by effectively removing real-time data fluctuations. The implementation of the extended Kalman filter (EKF) state of charge (SOC) estimation algorithm involves several critical steps to ensure accurate and efficient performance.

First, proper battery model selection and parameterization are essential. The 2RC equivalent circuit model (ECM) selected accurately represents the cell dynamics while maintaining computational performance. Second, it is important to correctly set the initial conditions and fine-tune the filter parameters. Process and measurement noise covariance is critical for the convergence and stability of the EKF. Third, the evaluation of model tolerances and solver settings (both fixed and variable) proved that fixed step settings and carefully selected tolerances are optimal, ensuring reliable performance without compromising accuracy.

Finally, it is important to consider the sampling time, as differences in intervals affect the accuracy of the SOC estimation. Taken together, these steps highlight the complexity of EKF implementation and the actions required to address it successfully.

The robust framework provided by this integration improves the performance and accuracy in battery parameter estimation, making the model especially suitable for online estimation in real-time applications, such as electric vehicles and other energy storage systems. With minimal computational complexity and a reduced need for large-scale training data, the EKF is proved to outperform traditional and other model-based approaches, positioning it as a highly viable solution to modern battery management challenges.

Author Contributions: Conceptualization, N.S.-M. and S.-V.S.; methodology, N.S.-M.; software, S.-V.S.; validation, S.-V.S. and N.S.-M.; formal analysis, N.S.-M. and S.-V.S.; investigation, N.S.-M. and S.-V.S.; resources, N.S.-M. data curation, N.S.-M.; writing—original draft preparation, S.-V.S.; writing—review and editing, S.-V.S. and N.S.-M.; visualization, S.-V.S.; supervision, M.B.; project administration, S.X.; funding acquisition, M.B. and S.X. All authors have read and agreed to the published version of the manuscript.

Funding: The experimental design of this research was funded by the French-German InnoTherms project.

Data Availability Statement: The raw data supporting the conclusions of this article will be made available by the authors on request.

Acknowledgments: The experimental setup was financially supported by the European Commission within the framework of the project InnoTherms. InnoTherms is part of an international co-operation project “AllFraTech”. The Cluster Electric Mobility Southwest intensifies its co-operation relations with relevant stakeholders in the Auvergne-Rhône-Alpes region through the cross-border cooperation project “Franco-German Alliance for Innovative Mobility Technologies (AllFraTech)”. The authors thank our colleagues Eric Mathieu and Serge Buathier from CETHIL for the experimental bench and acquisition software.

Conflicts of Interest: The authors declare no conflicts of interest.

References

1. Lu, L.; Han, X.; Li, J.; Hua, J.; Ouyang, M. A review on the key issues for lithium-ion battery management in electric vehicles. *J. Power Sources* **2013**, *226*, 272–288. [[CrossRef](#)]
2. Hannan, M.A.; Lipu, M.S.H.; Hussain, A.; Mohamed, A. A review of lithium-ion battery state of charge estimation and management system in electric vehicle applications: Challenges and recommendations. *Renew. Sustain. Energy Rev.* **2017**, *78*, 834–854. [[CrossRef](#)]
3. Wang, T.; Tseng, K.; Zhao, J.; Wei, Z. Thermal investigation of lithium-ion battery module with different cell arrangement structures and forced air-cooling strategies. *Appl. Energy* **2014**, *134*, 229–238. [[CrossRef](#)]
4. Hariharan, K.S. A coupled nonlinear equivalent circuit—Thermal model for lithium ion cells. *J. Power Sources* **2013**, *227*, 171–176. [[CrossRef](#)]
5. Akbarzadeh, M.; Kalogiannis, T.; Jaguemont, J.; Jin, L.; Karimi, D.; Beheshti, H.; Van Mierlo, J.; Bercibar, M. A comparative study between air cooling and liquid cooling thermal management systems for a high-energy lithium-ion battery module. *Appl. Therm. Eng.* **2021**, *198*, 117503. [[CrossRef](#)]
6. Saputra, L.H.; Haq, I.N.; Leksono, E.; Romadhon, R.; Kurniadi, D.; Yuliarto, B. Development of battery thermal management system for LiFeMnPO₄ module using air cooling method to minimize cell temperature differences and parasitic energy. In Proceedings of the 2017 4th International Conference on Electric Vehicular Technology (ICEVT), Bali, Indonesia, 2–5 October 2017; pp. 87–92.
7. Mahfoudi, N.; Boutaous, M.; Xin, S.; Buathier, S. Thermal Analysis of LMO/Graphite Batteries Using Equivalent Circuit Models. *Batteries* **2021**, *7*, 58. [[CrossRef](#)]
8. Hu, X.; Li, S.; Peng, H. A comparative study of equivalent circuit models for Li-ion batteries. *J. Power Sources* **2012**, *198*, 359–367. [[CrossRef](#)]
9. Li, Z.; Shi, X.; Shi, M.; Wei, C.; Di, F.; Sun, H. Investigation on the Impact of the HPPC Profile on the Battery ECM Parameters’ Offline Identification. In Proceedings of the 2020 Asia Energy and Electrical Engineering Symposium (AEEES), Chengdu, China, 29–31 May 2020; pp. 753–757.
10. Reshma, P.; Manohar, V.J. Collaborative evaluation of SoC, SoP and SoH of lithium-ion battery in an electric bus through improved remora optimization algorithm and dual adaptive Kalman filtering algorithm. *J. Energy Storage* **2023**, *68*, 107573. [[CrossRef](#)]

11. Li, J.; Peng, Y.; Wang, Q.; Liu, H. Status and Prospects of Research on Lithium-Ion Battery Parameter Identification. *Batteries* **2024**, *10*, 194. [[CrossRef](#)]
12. Shrivastava, P.; Soon, T.K.; Bin Idris, M.Y.I.; Mekhilef, S. Overview of model-based online state-of-charge estimation using Kalman filter family for lithium-ion batteries. *Renew. Sustain. Energy Rev.* **2019**, *113*, 109233. [[CrossRef](#)]
13. Rimsha; Murawwat, S.; Gulzar, M.M.; Alzahrani, A.; Hafeez, G.; Khan, F.A.; Abed, A.M. State of charge estimation and error analysis of lithium-ion batteries for electric vehicles using Kalman filter and deep neural network. *J. Energy Storage* **2023**, *72*, 108039. [[CrossRef](#)]
14. Kang, L.; Li Zhang, L. Science Direct. 2019. Available online: <https://pdf.sciencedirectassets.com/313346/1-s2.0-S2405896319X00130/1-s2.0-S2405896319307827/main.pdf?X-Amz-Security-Token=IQoJb3JpZ2luX2VjEH0aCXVzLWVhc3QtMSJHMEUCIFqxwf2MWPYyJ7IfGENeZ9rMqGjVeSjYHdYMLw/35wl1AiEA5le4jNDSOIOLsfYOKuDnPXqyCnUhnqKITgCuG7kZzG> (accessed on 23 April 2024).
15. Zhong, C.-M.; Li, G.-Y.; Zheng, X. Science Direct. 2024. Available online: <https://pdf.sciencedirectassets.com/783334/1-s2.0-S1452398124X00097/1-s2.0-S1452398124002888/main.pdf?X-Amz-Security-Token=IQoJb3JpZ2luX2VjEH0aCXVzLWVhc3QtMSJHMEUCIF8Kg4Fj+9qhZqRD3sA7Ey7GI8/e0u1vSpWWKZz5/QkHAiEArtPkum7A17L3I6iYH1O8NZCPc2JvuNkeseOj9> (accessed on 23 April 2024).
16. Zhao, X.; Sun, B.; Zhang, W.; He, X.; Ma, S.; Zhang, J.; Liu, X. Error theory study on EKF-based SOC and effective error estimation strategy for Li-ion batteries. *Appl. Energy* **2024**, *353*, 121992. [[CrossRef](#)]
17. Li, Y.; Ye, M.; Wang, Q.; Lian, G.; Xia, B. An Improved Model Combining Machine Learning and Kalman Filtering Architecture for State of Charge Estimation of Lithium-Ion Batteries. *Green Energy Intell. Transp.* **2024**, *3*, 100163. [[CrossRef](#)]
18. Monirul, I.M.; Qiu, L.; Ruby, R. Accurate SOC estimation of ternary lithium-ion batteries by HPPC test-based extended Kalman filter. *J. Energy Storage* **2024**, *92*, 112304. [[CrossRef](#)]
19. Taborelli, C.; Onori, S. State of charge estimation using extended Kalman filters for battery management system. In Proceedings of the 2014 IEEE International Electric Vehicle Conference (IEVC), Florence, Italy, 17–19 December 2014; pp. 1–8.
20. Jiang, S. A Parameter Identification Method for a Battery Equivalent Circuit Model. In Proceedings of the SAE 2011 World Congress & Exhibition, Detroit, MI, USA, 12–14 April 2011.
21. Plett, G.L. Kalman-Filter SOC Estimation for LiPB HEV Cells. Available online: <http://mocha-java.uccs.edu/dossier/RESEARCH/2002evs19b-.pdf> (accessed on 23 April 2024).
22. Made, R.I.; Lin, J.; Zhang, J.; Zhang, Y.; Moh, L.C.; Liu, Z.; Ding, N.; Chiam, S.Y.; Khoo, E.; Yin, X.; et al. Health diagnosis and recuperation of aged Li-ion batteries with data analytics and equivalent circuit modeling. *iScience* **2024**, *27*, 109416. [[CrossRef](#)] [[PubMed](#)]
23. Hwang, F.S.; Confrey, T.; Reidy, C.; Picovici, D.; Callaghan, D.; Culliton, D.; Nolan, C. Review of battery thermal management systems in electric vehicles. *Renew. Sustain. Energy Rev.* **2024**, *192*, 114171. [[CrossRef](#)]
24. Hu, X.; Zou, C.; Zhang, C. Technological Developments in Batteries: A Survey of Principal Roles, Types, and Management Needs. *IEEE Power Energy Mag.* **2017**, *15*, 20–31. [[CrossRef](#)]

Disclaimer/Publisher’s Note: The statements, opinions and data contained in all publications are solely those of the individual author(s) and contributor(s) and not of MDPI and/or the editor(s). MDPI and/or the editor(s) disclaim responsibility for any injury to people or property resulting from any ideas, methods, instructions or products referred to in the content.